Ceramics International xxx (xxxx) xxx–xxx

Contents lists available at ScienceDirect

Ceramics International

journal homepage: www.elsevier.com/locate/ceramint

Effect of Mg/B ratio and Sr^{2+} substitution for Mg^{2+} on the sintering, phase composition and microwave dielectric properties of $Mg_3B_2O_6$ ceramics

Yong-jun Gu[a,b,d,*], Xian-bing Ding[a], Wei Hu[a,b], Jin-liang Huang (Ph.D)[a,c,**], Qian Li[a], Li-hua Li[a], Xin-li Li[a], Xing-hua Yang[d], Min Chen (Ph.D)[e,***], Bok-hee Kim[a,f]

[a] School of Materials Science and Engineering, Henan University of Science and Technology, China
[b] Henan Key Laboratory of Materials Science & Processing Technology for Non-ferrous Metals, China
[c] Collaborative Innovation Center of Nonferrous Metals, Henan Province, China
[d] Henan Key Laboratory of Research for Central Plains Ancient Ceramics, Pingdingshan University, China
[e] School of Materials Science and Energy Engineering, Foshan University, China
[f] Department of Electronic Materials Engineering, Chonbuk National University, South Korea

ARTICLE INFO

Keywords:
Microwave dielectric ceramics
Dielectric property
Sintering
$Mg_3B_2O_6$

ABSTRACT

$Mg_3B_2O_6$ is a typical microwave dielectric ceramic with a high Qf value, but the pure $Mg_3B_2O_6$ ceramic is difficult to be obtained due to the volatilization of B_2O_3 resulting from the high temperature during the fabrication process. We reveal the effects of Mg/B ratio and Sr^{2+} substitution for Mg^{2+} on the phase composition, sintering behavior, microstructure, and microwave dielectric properties of $Mg_3B_2O_6$. The pure $Mg_3B_2O_6$ ceramic can be obtained with Mg/B ratio equal to 1.2. Proper excessive free-MgO is benefit to the improvement of Qf value of $Mg_3B_2O_6$, while it is detrimental to the densification of $Mg_3B_2O_6$. No second phase was detected in the Sr^{2+} substituted $Mg_3B_2O_6$ and excellent microwave dielectric properties (ε_r = 6.9, Qf = 110820 GHz, and τ_f = −32.4 ppm/°C at 12.8 GHz) were obtained in the $(Mg_{0.998}Sr_{0.002})_3B_2O_6$ (x = 0.2 mol.%) ceramic sample sintered at 1250 °C for 3h, making it a hopeful candidate for wireless communications. These results bring forward the underlying insights needed to direct the design of microwave dielectric ceramics with high Qf values for personal communication applications.

1. Introduction

Microwave dielectric ceramic is a new type of functional ceramic material which can be used at microwave circuits (mainly 300 MHz-300 GHz). It is commonly used as resonators, filters, phase shifters and substrates in microwave integrated circuits [1–5]. With the development of communication technology to 5G/6G, microwave components are developing towards miniaturization, chip and low cost. Low temperature co-fired ceramics (LTCC) technology has been widely used and requires that microwave dielectric materials must be co-fired with metal electrodes [6–8]. However, the sintering temperatures of ceramic materials are generally high [9,10]. At present, there are four common ways to reduce sintering temperature. (1) Adding sintering aids with low melting point/softening point, such as H_3BO_3 [11], $BaCu(B_2O_5)$ [12–14] and glasses [9,15], to improve the densification by liquid phase sintering mechanism. Although the sintering temperature of the ceramic material was effectively reduced, its microwave dielectric properties were deteriorated significantly. (2) Using ultra-fine powder to improve the driving force of sintering [16]. However, the sintering temperature reduction is limited, which still can't meet the application requirements of LTCC. (3) Special sintering methods, such as spark plasma sintering (SPS) [17]. However, complex and expensive equipment is needed in the material preparation process, which is not conducive to industrial promotion. (4) Developing materials with low sintering temperature [18–22].

MgO is widely used as a high temperature and heat-resistant material. Because of its excellent electrical insulation and high thermal conductivity, it can also be used as a substrate material. The thermal conductivity of MgO used as ceramic substrate is more than two times higher than that of alumina. However, the high sintering temperature limits its application in LTCC. It was reported that the sintering temperature of MgO can be significantly reduced by introducing B_2O_3. In

* Corresponding author. School of Materials Science and Engineering, Henan University of Science and Technology, China.
** Corresponding author. School of Materials Science and Engineering, Henan University of Science and Technology, China.
*** Corresponding author.
E-mail addresses: yjgu_ycs@126.com (Y.-j. Gu), huangjl@haust.edu.cn (J.-l. Huang), minchen1981@126.com (M. Chen).

https://doi.org/10.1016/j.ceramint.2020.07.073
Received 8 February 2020; Received in revised form 2 July 2020; Accepted 10 July 2020

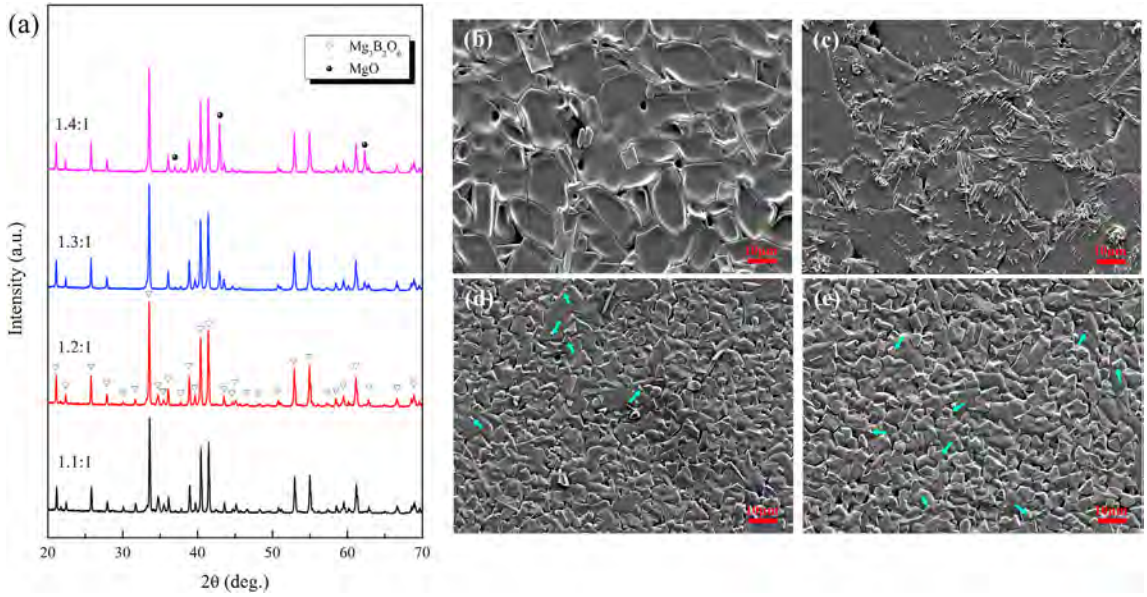

Fig. 1. (a) Typical XRD patterns of the MgO–B_2O_3 ceramic samples sintered at 1250 °C for 3h with different Mg/B ratios and (b–e) typical SEM images of the thermal etched surface of MgO–B_2O_3 ceramic samples sintered at 1250 °C for 3h with Mg/B ratio equal 1.1:1, 1.2:1, 1.3:1, and 1.4:1, respectively.

the binary system of B_2O_3–MgO, the stable compounds are $Mg_3B_2O_6$ (1400 °C), $Mg_2B_2O_5$ (1381 °C) and MgB_2O_4 (1193 °C) [23]. Mori et al. [24] found that $Mg_3B_2O_6$ (kotoite) has good microwave dielectric properties in the study of new glass ceramics for LTCC. However, $Mg_3B_2O_6$ is easy to decompose into MgO and $Mg_2B_2O_5$ in the process of heating, which results in deteriorations of its sinterability and dielectric properties. In addition, in the process of $Mg_3B_2O_6$ calcination/sintering at high temperature, the volatilization of B_2O_3 will cause serious deviation from the nominal composition. Although the densification of $Mg_3B_2O_6$ at 950 °C can be achieved by adding Li_2O–MgO–B_2O_3–SiO_2 glass as sintering assistant, its dielectric properties are significantly deteriorated, and its optimal Qf value is only 21000 GHz (at 6.5 GHz) [5]. In addition, proper ion substitution, especially elements with similar properties such as congeneric elements is beneficial to the improvement of densification and dielectric properties. For example, Song et al. [25] fabricated $(Mg_{1-x}Sr_x)_2Al_4Si_5O_{18}$ (MS_xAS) ceramics by traditional sintering method and found that the densification of the MS_xAS ceramic with x equal 0.2 was dramatically enhanced and a evident increasing of Qf value from 24100 GHz to 38900 GHz (at ~13 GHz) was also obtained. In this paper, a simple method was presented for the preparation of single phase $Mg_3B_2O_6$ ceramic by adjusting the Mg/B ratio. The effects of Mg/B ratio and Sr^{2+} substitution for Mg on the phase composition, sintering, microstructure, and dielectric properties of $Mg_3B_2O_6$ were also studied in details.

2. Experimental

$Mg_3B_2O_6$ samples were prepared by solid state reaction. The analytical pure MgO (98.5%) and H_3BO_3 (99.5%) were purchased from Sinopharm Chemical Reagent Co., Ltd. In order to investigate the effect of Mg/B ratio on the phase composition and dielectric properties of $Mg_3B_2O_6$, Mg/B ratio equal to 1.4:1,1.3:1,1.2:1,1.1:1 were selected in the batch. The MgO and H_3BO_3 with different proportion are weighed and then poured into nylon tank for ball milling for 4h. The slurry is dried and calcined at 1100 °C for 3h. The calcined powder is milled again and then granulated with PVA. Then it is pressed into a cylinder with a diameter of 11 mm and a height of 5–6 mm. These cylinders were sintered at 1250 °C for 3h.

The $(Mg_{1-x}Sr_x)_3B_2O_6$ ceramics were also prepared by solid-state reaction method. The raw materials were high-purity MgO (98.5%), $SrCO_3$ (99.0%), H_3BO_3 (99.5%), purchased from Sinopharm Chemical Reagent Co., Ltd. According to x (0, 0.1%, 0.2%, 0.5% and 1 mol.%), the above raw materials are weighed and put into Nylon tank, for ball milling with zirconia ball and anhydrous ethanol for 4h, dried at 100 °C and then calcined at 1100 °C for 3h. The calcined powder is crushed and milled again, dried, and then added to PVA for granulation. It is compressed into a cylindrical block with a diameter of 11 mm and a height of 5–6 mm under uniaxial pressure, and then put into a muffle furnace for sintering at 1200–1250 °C for 3h.

The bulk densities of as-fabricated ceramic samples are characterized by Archimedes drainage method. The phase compositions of the calcined powder sample and the sintered ceramic samples were analyzed by X-ray diffractometer (D8 advance X-ray analyzer, Cu target, Kα, wavelength 0.15406 nm) with the scanning angle between 20 and 70°. Scanning electron microscope (JEOL JSM-7800F) was used to observe the thermal etched surface of the sintered ceramic sample. Before the observations, smart coater (JEOL DII-29030SCTR) was used to sputter gold on the thermal etched surface of the ceramic samples, so as to reduce the adverse effect of electronic agglomeration caused by the poor conductivity of the sample. The closed cavity method is used to measure the microwave dielectric properties of the samples by using vector network analyzer (Agilent N5230C-220PNA-L), and the resonance frequencies at 20 and 80 °C were measured respectively, and then the temperature coefficient of resonance frequency between 20-80 °C is calculated by equation (1).

$$\tau_f = \frac{f_{80} - f_{20}}{f_{20} \times (80 - 20)} \times 10^6 (ppm/^oC) \quad (1)$$

where f_{80} and f_{20} represent the resonant frequencies at 80 °C and 20 °C, respectively.

3. Results and discussion

Fig. 1(a) shows the typical XRD patterns of MgO–B_2O_3 ceramic samples sintered at 1250 °C for 3h with different Mg/B ratios. In the binary system of B_2O_3–MgO, the stable compounds are $Mg_3B_2O_6$ (1400 °C), $Mg_2B_2O_5$ (1381 °C) and MgB_2O_4 (1193 °C) [23]. Due to the volatilization of B_2O_3, excessive B_2O_3/H_3BO_3 was usually added in the ceramics containing B_2O_3 or H_3BO_3 [26–28], such as $NiTiNb_2O_8$–B_2O_3 [28] and $MgZrNb_2O_8$–H_3BO_3 [3]. In this study, when the Mg/B ratio is 1.4, the sintered samples are mainly composed of $Mg_3B_2O_6$ phase and a small amount of free MgO (marked by the blue arrows in Fig. 1e),

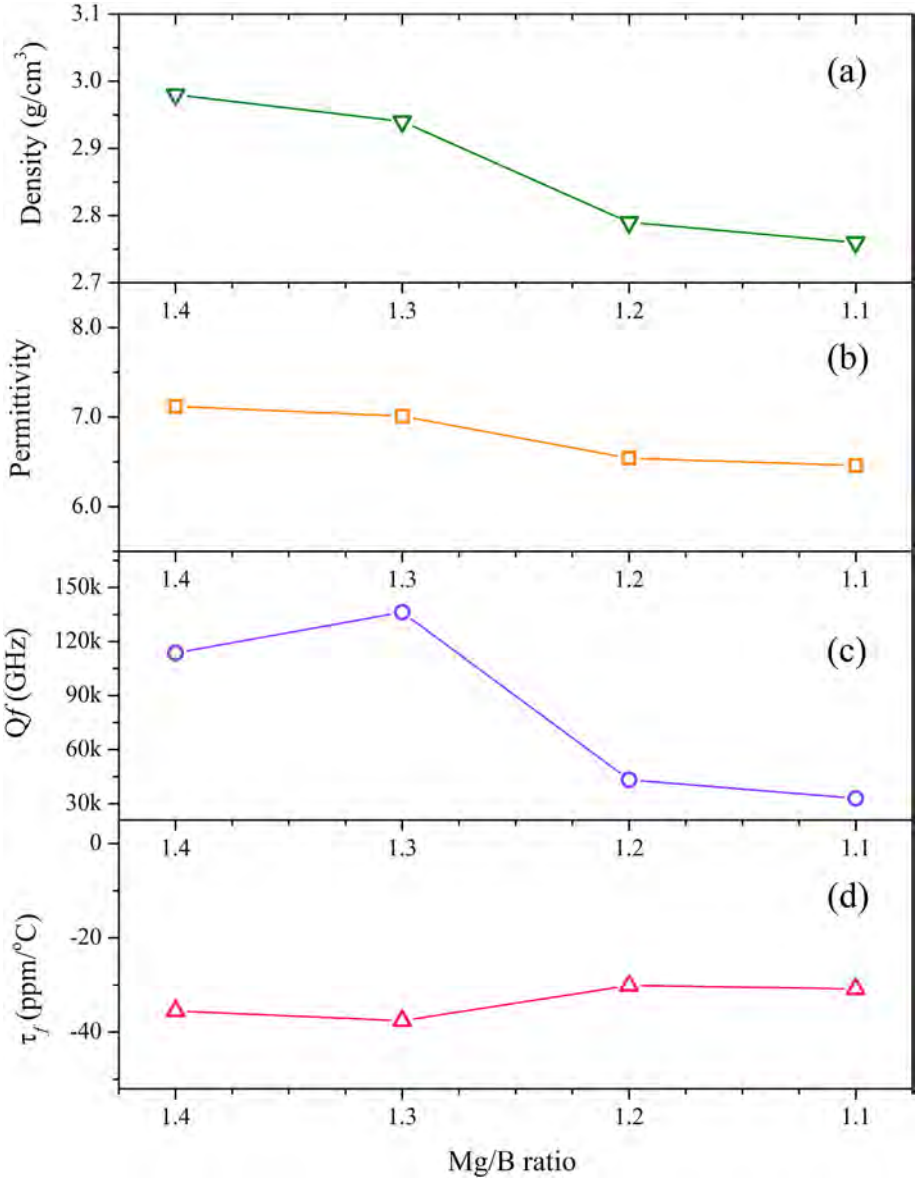

Fig. 2. (a) Densities, (b) permittivities, (c) Q*f*, and (d) temperature coefficients of resonant frequency (τ_f) of the MgO–B_2O_3 ceramic samples sintered at 1250 °C for 3h with different Mg/B ratios.

which shows that the excessive H_3BO_3 is not enough to make up for the high temperature volatilization of B_2O_3. When Mg/B decreased to 1.3, the free-MgO (marked by the blue arrow in Fig. 1d) still remains in the sample. When Mg/B is 1.2, the sample is a single phase $Mg_3B_2O_6$ after sintering at 1250 °C for 3h. Fig. 1(b-e) shows typical SEM images of the thermal etched surface of MgO–B_2O_3 ceramic samples sintered at 1250 °C for 3h with Mg/B ratio equal 1.1:1, 1.2:1, 1.3:1, and 1.4:1, respectively. It can be clearly seen that all the as-fabricated ceramic samples have dense microstructures and the grain sizes of the ceramic samples with Mg/B ratio equal 1.1:1 and 1.2:1 are much larger those of the samples with Mg/B = 1.3 and 1.4, which indicates that more B_2O_3 is beneficial to the grain growth. Fig. 2(a) shows the bulk densities of the MgO–B_2O_3 ceramic samples sintered at 1250 °C for 3h. With the decrease of Mg/B ratio from 1.4 to 1.1, the bulk densities of sintered samples decrease monotonously. As mentioned before, the stable compounds in MgO–B_2O_3 binary system are $Mg_3B_2O_6$, $Mg_2B_2O_5$ and MgB_2O_4. Their theoretical densities are 3.04, 2.91, and 2.53 g/cm^3, respectively. In addition, the theoretical density of MgO is 3.57 g/cm^3. When Mg/B ratio is 1.4 and 1.3, $Mg_3B_2O_6$ and MgO phase (marked by the blue arrows in Fig. 1d-e) coexist in the sintered ceramic samples, and the content of MgO phase in the former is higher than that in the latter. In addition, with the Mg/B ratio reduced to 1.1, $Mg_2B_2O_5$ phase with lower theoretical density appears, which leads to further reduction of bulk density of sintered samples.

Fig. 2(b-d) show the microwave dielectric properties of the MgO–B_2O_3 ceramic samples sintered at 1250 °C for 3h as a function of Mg/B ratio. As illustrated in Fig. 2(b), the change trend of permittivities of the sintered sample with Mg/B ratio is similar to that of bulk density, which indicates that the bulk densities, to some extent, determine the permittivities of the as-fabricated ceramic samples. When Mg/B ratio decreases from 1.4 to 1.1, the permittivities decrease monotonously from 7.1 to 6.4, while the Q*f* value (at ~13 GHz) increase first and reach the maximum (136302 GHz) at 1.3, and then decrease to 32994 GHz. Generally speaking, the Q*f* value of a material is not only related to its intrinsic properties, but also related to the external factors such as grain boundaries, pores, defects and so on [29]. In this study, when the Mg/B ratio is reduced from 1.4 to 1.3, the content of free MgO decreases monotonously, which is conducive to the densification of MgO–B_2O_3 samples (as illustrated in Fig. 1d and Fig. 2a) and results in the increase of Q*f* value of sintered samples. The Q*f* value of MgO is as

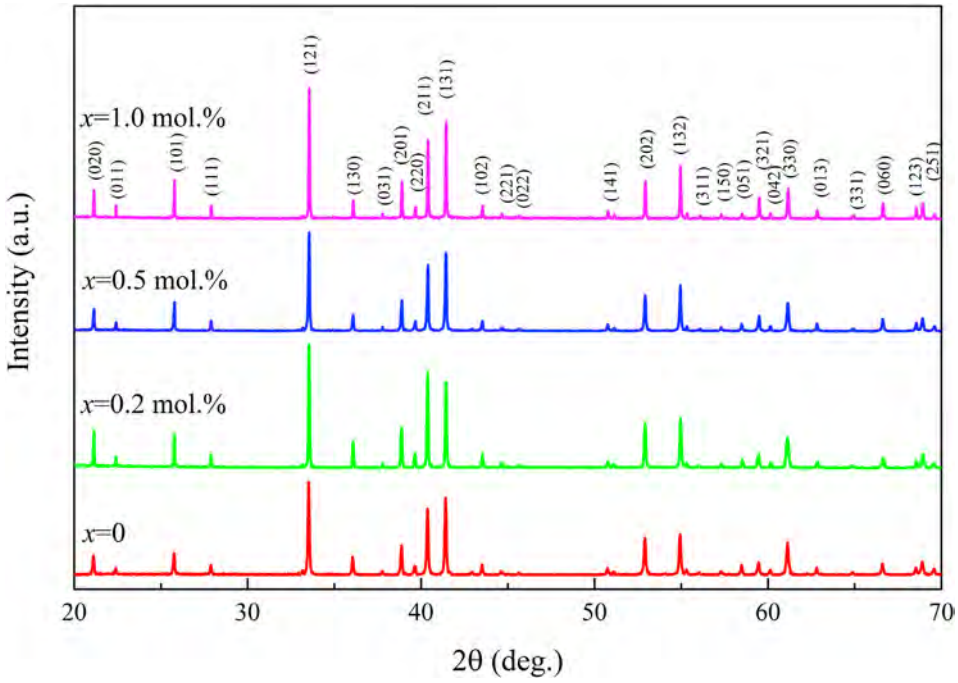

Fig. 3. Typical XRD patterns of the $(Mg_{1-x}Sr_x)_3B_2O_6$ (x = 0–1.0 mol.%) ceramic samples sintered at 1250 °C for 3h.

high as 670000 GHz [30]. When Mg/B is 1.2, the corresponding sintered sample is only single-phase $Mg_3B_2O_6$ and no free-MgO is detected, which results in the sharp drop of Qf value. With Mg/B further reduced to 1.1, the Qf value of the corresponding sample further decreased. In addition, in the process of Mg/B ratio change from 1.4 to 1.1, the temperature coefficients of resonant frequency (τ_f) of the sintered MgO–B_2O_3 ceramic samples sintered at 1250 °C for 3h have little change, between −30.1 and −37.6 ppm/°C.

In order to investigate the effect of Sr^{2+} substitution for Mg^{2+} on $Mg_3B_2O_6$, the ceramic samples with Mg//B equal to 1.2 is selected below due to single phase and the higher Qf value. Fig. 3 shows the typical XRD patterns of the $(Mg_{1-x}Sr_x)_3B_2O_6$ (x = 0–1.0 mol.%) ceramic samples sintered at 1250 °C for 3h as a function of Sr^{2+} substitution. It can be seen from Fig. 3 that the undoped ceramic (x = 0) is a pure $Mg_3B_2O_6$ phase (JCPDS 75–1807), which corresponds to an orthorhombic system, a spatial group Pnmn (No.58). No diffraction peak corresponding to second phase was detected in all the Sr-substituted $(Mg_{1-x}Sr_x)_3B_2O_6$ (x = 0–1.0 mol.%). It is reported that during the synthesis of $Mg_3B_2O_6$, $Mg_2B_2O_5$ (local B_2O_3 enrichment) and/or free MgO (local B_2O_3 deficiency) are easy to be produced. When a small amount of Sr^{2+} is added, the segregation of B_2O_3 in the sample is reduced. Accordingly, a single-phase $(Mg_{1-x}Sr_x)_3B_2O_6$ ($x \leq$ 1.0 mol.%) solid solution is formed, indicating that the substitution of Sr^{2+} for Mg^{2+} does not affect the phase composition of $Mg_3B_2O_6$.

Fig. 4A-E shows the typical SEM images of the thermal etched surfaces of $(Mg_{1-x}Sr_x)_3B_2O_6$ (x = 0, 0.1%, 0.2%, 0.5%, and 1.0 mol.%) ceramics sintered at 1250 °C for 3h. As presented in Fig. 4A, the pure $Mg_3B_2O_6$ shows a relatively dense compact and the grain size is small. Compared with it, the grain size of $(Mg_{1-x}Sr_x)_3B_2O_6$ ceramics increases obviously after Sr^{2+} substitution. In addition, the grain size of $(Mg_{1-x}Sr_x)_3B_2O_6$ increases with the increment of Sr^{2+} substitution. Moreover, the more Sr^{2+} substitution, the larger grain size. It may be that the grain boundary migration rate of $(Mg_{1-x}Sr_x)_3B_2O_6$ increases after the introduction of Sr^{2+}. To clarify this more clearly, the area scan EDS analysis of the thermal etched surfaces was carried out to confirm the distribution of Sr^{2+} in the sintered $(Mg_{1-x}Sr_x)_3B_2O_6$ (x = 0, 0.2%, 0.5%, and 1.0 mol.%) ceramic sample. Fig. 4F-I shows the EDS layered image and the element distribution of Sr, Mg, and O corresponding to $(Mg_{1-x}Sr_x)_3B_2O_6$ (x = 1.0 mol.%) ceramic sample, respectively. The Mg and O element show homogenous distribution (Fig. 4M, I), while Sr element shows an enrichment at the grain boundary (Fig. 4S). Furthermore, the $(Mg_{0.998}Sr_{0.002})_3B_2O_6$ (x = 0.2 mol.%) ceramic sample has larger and uniform grains, cleaner grain boundaries, more homogenous distribution of Sr^{2+} (Fig. 4C), which are beneficial to its microwave dielectric properties, especially its Qf value.

Fig. 5 shows the relative densities and permittivities of $(Mg_{1-x}Sr_x)_3B_2O_6$ (x = 0, 0.1%, 0.2%, 0.5% mol.%) ceramics sintered at 1200–1250 °C for 3h as a function of Sr^{2+} substitution. The bulk density of pure $Mg_3B_2O_6$ ceramics is 2.95 g/cm^3 (the corresponding relative density is 95.6%), which is similar to that of the samples sintered at 1350 °C for 4h by Kan et al. [30]. Compared with pure $Mg_3B_2O_6$, the theoretical density of $(Mg_{1-x}Sr_x)_3B_2O_6$ remained almost unchanged after doping a small amount of Sr^{2+}. However, due to the substitution of Sr^{2+} for Mg^{2+}, the mean grain sizes become much larger and some pores trapped in the grains and abnormal-grew grains (see Fig. 4A-F) occur, most likely because of the significantly accelerated grain boundary migration of $(Mg_{1-x}Sr_x)_3B_2O_6$ during the sintering process. The relative density of $(Mg_{1-x}Sr_x)_3B_2O_6$ sintered samples decreases with the increment of Sr^{2+} substitution. In addition, the sintering temperature also has a certain influence on the relative density of $Mg_3B_2O_6$, as shown in Fig. 5. When the amount of Sr^{2+} substitution is the same, such as x = 0.2, the relative density corresponding to 1225 °C is the largest (96.1%), which further shows that the sintering activity of $Mg_3B_2O_6$ increases with the amount of Sr^{2+} substitution. For a ceramic material, the permittivity, to some extent, is determined by its relative density. As illustrated in Fig. 5, the change trend of the permittivities of the as-sintered $(Mg_{1-x}Sr_x)_3B_2O_6$ ceramic samples is similar to that of relative density. Under the investigated experimental conditions (sintering temperature ~1200–1250 °C and $x \leq$ 1.0 mol.%), the relative densities of as-fabricated $(Mg_{1-x}Sr_x)_3B_2O_6$ ceramic samples are all above 90%, accordingly the corresponding permittivities change little with sintering temperature and Sr^{2+} substitution amount, basically between 6.6 and 7.0.

Fig. 6 shows the Qf values and temperature coefficients of resonant frequency of $(Mg_{1-x}Sr_x)_3B_2O_6$ (x = 0–1.0 mol.%) ceramic samples sintered at 1200–1250 °C for 3h as a function of Sr^{2+} substitution. Generally speaking, the Qf value of a material is not only related to its intrinsic properties, but also related to the external factors such as grain

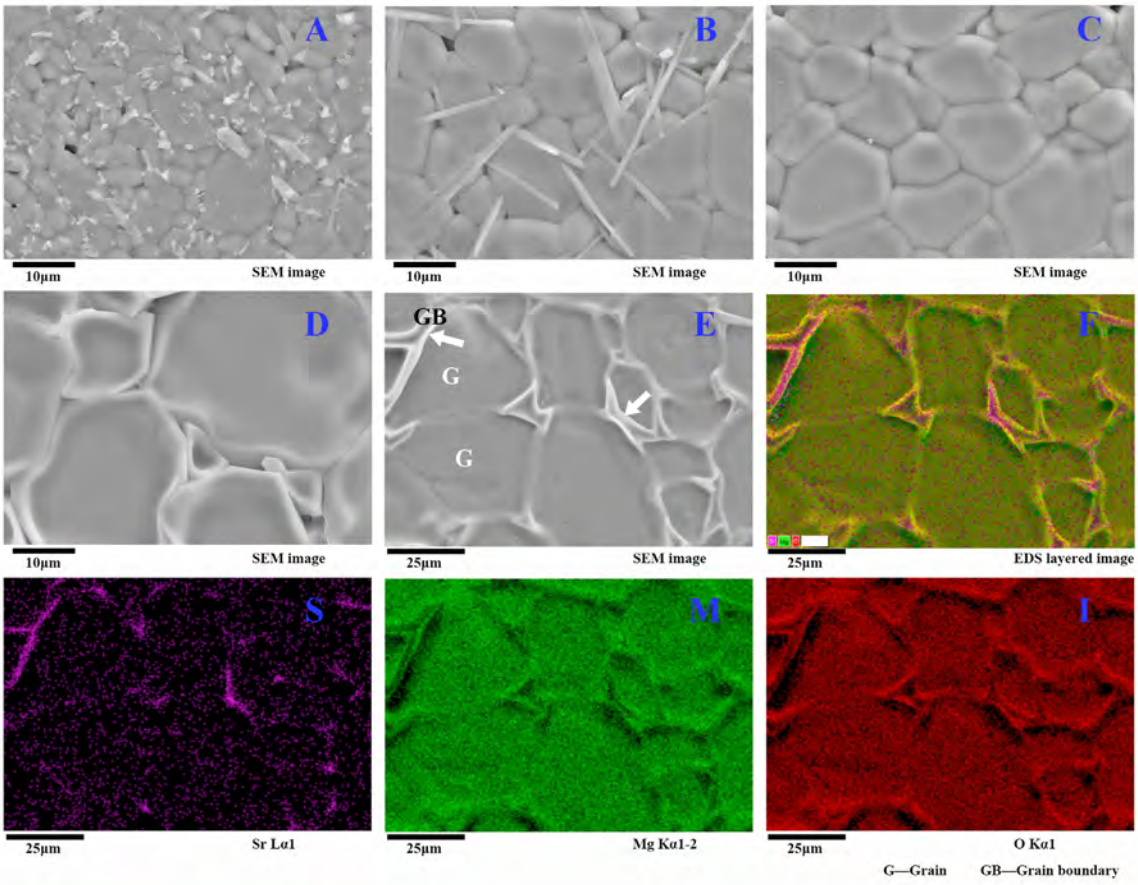

Fig. 4. (A–F) Typical SEM images of the thermal etched surfaces of $(Mg_{1-x}Sr_x)_3B_2O_6$ (x = 0, 0.1%, 0.2%, 0.5%, and 1.0 mol.%) ceramics sintered at 1250 °C for 3h; (F–I) EDS layered image and element distribution of Sr, Mg, and O corresponding to $(Mg_{1-x}Sr_x)_3B_2O_6$ (x = 1.0 mol.%) ceramic sample sintered at 1250 °C for 3h, respectively.

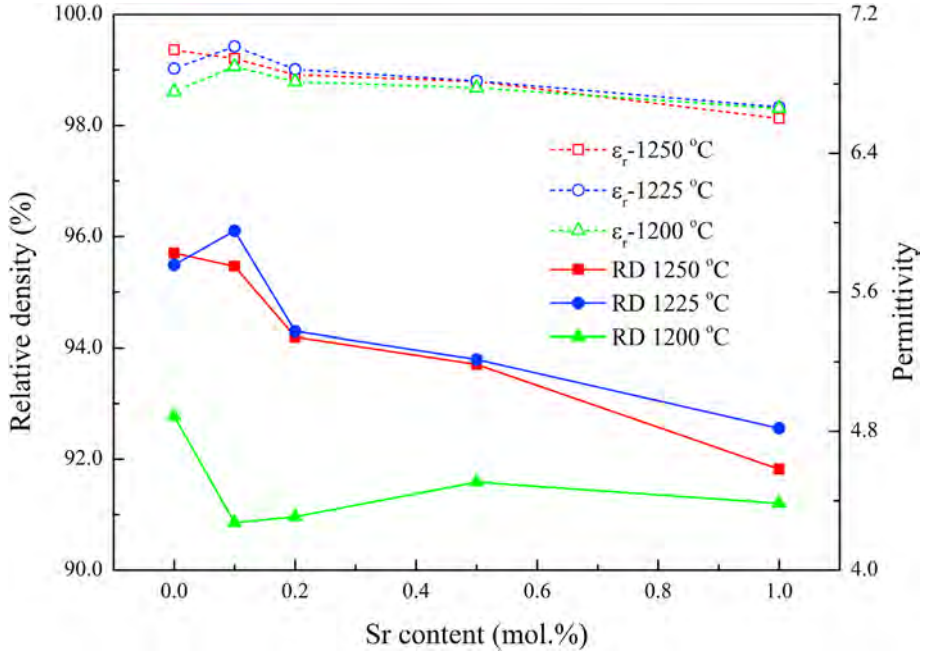

Fig. 5. Relative densities and permittivities of the $(Mg_{1-x}Sr_x)_3B_2O_6$ (x = 0–1.0 mol.%) ceramic samples sintered at 1200–1250 °C for 3h.

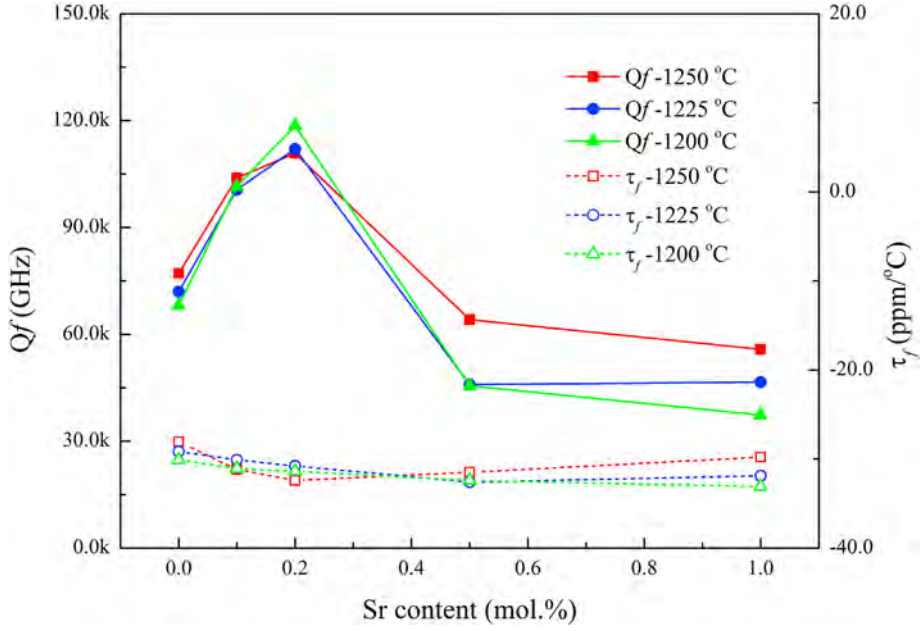

Fig. 6. *Qf* and temperature coefficients of resonant frequency (τ_f) of the $(Mg_{1-x}Sr_x)_3B_2O_6$ (x = 0–1.0 mol.%) ceramic samples sintered at 1200–1250 °C for 3h.

boundaries, pores, defects and so on. When the substitution of Sr^{2+} for Mg^{2+} increases from 0 to 1.0 mol.%, the *Qf* values of the sintered ceramic sample increase first, saturate at x = 0.2 mol.%, and then decrease quickly. As mentioned above, the $(Mg_{0.998}Sr_{0.002})_3B_2O_6$ (x = 0.2 mol.%) ceramic sample has larger and uniform grains, cleaner grain boundaries, more homogenous distribution of Sr^{2+} (Fig. 4C), which are beneficial to its microwave dielectric properties, especially its *Qf* value. In addition, the *Qf* values of the $(Mg_{0.998}Sr_{0.002})_3B_2O_6$ (x = 0.2 mol.%) ceramic samples decrease slightly with the sintering temperature increasing from 1200 °C to 1250 °C. The reason for the above results may be that, on the one hand, the lattice distortion and other defects of $Mg_3B_2O_6$ increase with the Sr^{2+} substitution for Mg^{2+}, which is harmful to its *Qf* values; on the other hand, the higher sintering activity of $Mg_3B_2O_6$ is conducive to the densification of the sample, resulting in the improvement of the quality factor. Furthermore, the temperature coefficients of resonant frequency of all the $(Mg_{1-x}Sr_x)_3B_2O_6$ (x = 0–1.0 mol.%) ceramic samples sintered at 1200–1250 °C is between −28.0 and −33.1 ppm/°C and the deviations is very little. This indicates that under the experimental conditions in this study, Sr^{2+} substitution for Mg^{2+} and sintering temperature have little effect on the temperature coefficients of resonant frequency. In short, the optimal microwave dielectric properties (ε_r = 6.9, *Qf* = 110820 GHz, and τ_f = −32.4 ppm/°C at 12.8 GHz) were obtained in the $(Mg_{0.998}Sr_{0.002})_3B_2O_6$ (x = 0.2 mol.%) ceramic samples sintered at 1250 °C, making it a hopeful candidate for wireless communications.

4. Conclusions

Microwave dielectric ceramics $(Mg_{1-x}Sr_x)_3B_2O_6$ (x = 0–1.0 mol.%) were prepared by solid state method. The effects of Mg/B ratio and Sr^{2+} substitution for Mg^{2+} on the phase composition, microstructure, sintering behavior and microwave dielectric properties of $(Mg_{1-x}Sr_x)_3B_2O_6$ (x = 0–1.0 mol.%) ceramics were investigated. Single phase $Mg_3B_2O_6$ ceramics was obtained when the Mg/B ratio is 1.2. Some free-MgO was detected when Mg/B ratio is 1.4 and 1.3, which is favorable to the improvement of *Qf* values. In addition, the substitution of Sr^{2+} for Mg^{2+} enhances the densification and grain growth of $(Mg_{1-x}Sr_x)_3B_2O_6$ (x = 0–1.0 mol.%) ceramics sintered at 1200–1250 °C for 3h. All the Sr^{2+} substituted ceramic samples exhibit single orthorhombic $Mg_3B_2O_6$ phase (JCPDS75-1807) and no diffraction peaks corresponding to second phase was detected. Excellent microwave dielectric properties (ε_r = 6.9, *Qf* = 110820 GHz, and τ_f = −32.4 ppm/°C at 12.8 GHz) were obtained in the $(Mg_{0.998}Sr_{0.002})_3B_2O_6$ (x = 0.2 mol.%) ceramic sample sintered at 1250 °C for 3h, making it a hopeful candidate for personal communications in 5G/6G.

Declaration of competing interest

The authors declare that they have no known competing financial interests or personal relationships that could have appeared to influence the work reported in this paper.

Acknowledgements

This work was supported by Henan Key Laboratory of Research for Central Plains Ancient Ceramics, Pingdingshan University (ZYGTCXW2018-02, ZYGTCKF201902, ZYGTCKF201903). The authors also acknowledged the kind help in the FESEM characterization by Dr. Li.

References

[1] K. Wang, H. Zhou, X. Liu, W. Sun, X. Chen, H. Ruan, A lithium aluminium borate composite microwave dielectric ceramic with low permittivity, near-zero shrinkage, and low sintering temperature, J. Eur. Ceram. Soc. 39 (2019) 1122–1126.
[2] J. Ren, K. Bi, X. Fu, Z. Peng, Microstructure and microwave dielectric properties of Al_2O_3 added $Li_2ZnTi_3O_8$ ceramics, Ceram. Int. 44 (2018) 8928–8933.
[3] H.T. Wu, J.D. Guo, J.X. Bi, Q.J. Mei, Effect of H_3BO_3 addition on the sintering behavior and microwave dielectric properties of wolframite-type $MgZrNb_2O_8$ ceramics, J. Alloys Compd. 661 (2016) 535–540.
[4] Z. Qing, B. Li, H. li, Y. Li, S. Zhang, Fabrication and properties of Li_2O–Al_2O_3–SiO_2 glass/Al_2O_3 composites for low temperature co-fired ceramic applications, J. Mater. Sci. Mater. Electron. 26 (2015) 1789–1794.
[5] G. Dou, M. Guo, Y. Li, J. Lin, The effect of LMBS glass on the microwave dielectric properties of the $Mg_3B_2O_6$ for LTCC, J. Mater. Sci. Mater. Electron. 26 (2015) 4207–4211.
[6] J. Raynaud, V. Pateloup, M. Bernard, D. Gourdonnaud, D. Passerieux, D. Cros, V. Madrangeas, T. Chartier, Hybridization of additive manufacturing processes to build ceramic/metal parts: example of LTCC, J. Eur. Ceram. Soc. 40 (2020) 759–767.
[7] Z. Weng, Z. Han, F. Xiao, H. Xue, D. Peng, Low temperature sintering and microwave dielectric properties of $Zn_{1.8}SiO_{3.8}$ ceramics with $BaCu(B_2O_5)$ additive for LTCC applications, Ceram. Int. 44 (2018) 14145–14150.
[8] H. Zuo, X. Tang, H. Guo, Q. Wang, C. Dai, H. Zhang, H. Su, Effects of $BaCu(B_2O_5)$

addition on microwave dielectric properties of Li_2TiO_3 ceramics for LTCC applications, Ceram. Int. 43 (2017) 13913–13917.
[9] H. Mao, X. Chen, F. Wang, W. Zhang, Effects of alkaline earth oxides on the densification and microwave properties of low-temperature fired $BaO–Al_2O_3–SiO_2$ glass–ceramic/Al_2O_3 composites, J. Mater. Sci. 54 (2019) 12371–12380.
[10] J. Chameswary, S. Thomas, M.T. Sebastian, Microwave dielectric properties of $Co_2La_4Ti_3Si_4O_{22}$ ceramics, J. Am. Ceram. Soc. 93 (2010) 1863–1865.
[11] J.X. Bi, C.F. Xing, X.S. Jiang, C.H. Yang, H.T. Wu, Low temperature sintering and microwave dielectric properties of $CoZrNb_2O_8$ ceramics with H_3BO_3 addition, J. Mater. Sci. Mater. Electron. 27 (2016) 6564–6569.
[12] Y.-J. Gu, C. Li, J.-L. Huang, Q. Li, L.-H. Li, X.-L. Li, Effect of $BaCu(B_2O_5)$ on the sintering and microwave dielectric properties of $Ca_{0.4}Li_{0.3}Sm_{0.05}Nd_{0.25}TiO_3$ ceramics, J. Eur. Ceram. Soc. 37 (2017) 4673–4679.
[13] R.-L. Jia, H. Su, X.-L. Tang, Y.-L. Jing, Effects of $BaCu(B_2O_5)$ addition on sintering temperature and microwave dielectric properties of $Ba_5Nb_4O_{15}$-$BaWO_4$ ceramics, Chin. Phys. B 23 (2014).
[14] H. Zhou, X. Liu, X. Chen, L. Fang, H. Wang, Microwave dielectric properties and compatibility with silver of low-fired $Ba_2Ti_3Nb_4O_{18}$ ceramics with $BaCu(B_2O_5)$ addition, J. Mater. Sci. 23 (2012) 238–242.
[15] D.-X. Zhou, F. Sun, Y.-X. Hu, Q.-Y. Fu, G. Dou, Low-temperature sintering and microwave dielectric properties of $Mg_3B_2O_6$-LMZBS composites, J. Mater. Sci. Mater. Electron. 23 (2012) 981–989.
[16] B. Fang, X. Lu, S. Zhang, N. Yuan, J. Ding, X. Zhao, F. Wang, Y. Tang, W. Shi, H. Xu, H. Luo, Decreasing sintering temperature for BCZT lead-free ceramics prepared via hydrothermal route, Funct. Mater. Lett. 10 (2017) 1750046.
[17] V.R. Mudinepalli, W.-C. Lin, S.H. Song, B.S. Murty, Spark plasma sintering temperature effect on structural, dielectric and ferroelectric properties of $Ba_{0.9}Sr_{0.1}TiO_3$ nanocrystalline ceramics, J. Electron. Mater. 44 (2015) 4308–4315.
[18] G.-Q. Zhang, J. Guo, L. He, D. Zhou, H. Wang, J. Koruza, M. Kosec, Preparation and microwave dielectric properties of ultra-low temperature sintering ceramics in $K_2O–MoO_3$ binary system, J. Am. Ceram. Soc. 97 (2014) 241–245.
[19] L. Li, W.B. Hong, X.J. Yan, X.M. Chen, Preparation and microwave dielectric properties of B_2O_3 bulk, Int. J. Appl. Ceram. Technol. 16 (2019) 2047–2052.
[20] X.B. Ding, Y.J. Gu, Q. Li, B.H. Kim, Q.F. Wang, J.L. Huang, Room temperature densified H_3BO_3 microwave dielectric ceramics with ultra-low permittivity and high quality factor for dielectric substrate applications, Ceram. Int. 46 (2020) 13225–13232.
[21] D. Zhou, L.-X. Pang, H.-D. Xie, J. Guo, B. He, Z.-M. Qi, T. Shao, X. Yao, C.A. Randall, Crystal structure and microwave dielectric properties of an ultralow-temperature-fired $(AgBi)_{0.5}WO_4$ ceramic, Eur. J. Inorg. Chem. (2014) 296–301 2014.
[22] W.B. Hong, L. Li, H. Yan, S.Y. Wu, H.S. Yang, X.M. Chen, Room-temperature-densified H_3BO_3 microwave dielectric ceramics with ultra-low permittivity and ultra-high Qf value, J. Materiomics 6 (2020) 233–239.
[23] T. Mutluer, M. Timucin, Phase equilibria in the system $MgO-B_2O_3$, J. Am. Ceram. Soc. 58 (1975) 196–197.
[24] N. Mori, Y. Sugimoto, J. Harada, Y. Higuchi, Dielectric properties of new glass-ceramics for LTCC applied to microwave or millimeter-wave frequencies, J. Eur. Ceram. Soc. 26 (2006) 1925–1928.
[25] M. Dang, H. Ren, T. Xie, X. Yao, H. Lin, L. Luo, Effects of B_2O_3 additive on ultra-low-loss $Mg_4Ta_2O_9$ microwave dielectric ceramics, J. Mater. Sci. Mater. Electron. 29 (2018) 568–572 26.
[26] K.-X. Song, Y.-Q. Yang, P. Zhang, J.-M. Xu, H.-B. Qin, Microstructures and microwave dielectric properties of $(Mg_{1-x}Sr_x)_2Al_4Si_5O_{18}$ ceramics, J. Inorg. Mater. 27 (2012) 575–579 25.
[27] Z. Qing, The effects of B_2O_3 on the microstructure and properties of lithium aluminosilicate glass-ceramics for LTCC applications, Mater. Lett. 212 (2018) 126–129.
[28] M. Wu, J. Chen, Y. Zhang, Effect of B_2O_3 addition on the microwave dielectric properties of $NiTiNb_2O_8$ ceramics, J. Mater. Sci. Mater. Electron. 29 (2018) 13132–13137.
[29] Y.-J. Gu, J.-L. Huang, Q. Li, X.-M. Ning, L.-H. Li, X.-L. Li, A novel low-fired and high-ε_r microwave dielectric ceramic $BaCu(B_2O_5)$-added $0.6Ca_{3/5}La_{4/15}TiO_3$-$0.4Li_{1/2}Nd_{1/2}TiO_3$, J. Mater. Sci. Mater. Electron. 29 (2018) 11378–11383.
[30] A. Kan, H. Ogawa, M. Sumino, M. Nishizuka, E. Suzuki, Microwave dielectric properties of xMgO-(1-x)B_2O_3 ceramics, Jpn. J. Appl. Phys. 48 (2009) 09KE03.